Erzincan Üniversitesi
Fen Bilimleri Enstitüsü Dergisi
2023, 16(3), 643-653
ISSN: 1307-9085, e-ISSN: 2149-4584
Araştırma Makalesi

Erzincan University
Journal of Science and Technology
2023, 16(3), 643-653
DOI: 10.18185/erzifbed.1234111
Research Article

The Effect of the Distance Between Unit Cells on the Frequency Stability of Frequency Selective Surfaces

Bora DÖKEN[1*]

[1] Elektrik Elektronik Fakültesi, İstanbul Teknik Üniversitesi, Maslak 34469, İstanbul, Türkiye

Received:15/01/2023, **Revised:**22/06/2023 , **Accepted:**14/09/2023 , **Published:** 31/12/2023

Abstract

Periodic conductive geometries that exhibit filtering behavior are referred to as frequency-selective surfaces (FSSs) in the literature. The frequency response of FSSs depends on their geometries, the angle of incidence, frequency, and polarization of the incoming electromagnetic wave. The distance "g" between periodic conductor geometries is an essential parameter for FSSs. However, the effect of this parameter on the frequency stability of FSSs has not been sufficiently investigated. Four different FSS geometries are selected to reveal this effect in this work. Simulations of these FSS geometries were carried out by Ansoft HFSS software. The most important result obtained from the FSS geometries is that when the distance between periodic conductor geometries is reduced below the 0.1 resonance wavelength, contrary to expectations, the incidence angle stability of the FSS is significantly reduced. The interference effect between different places on the conductor paths of neighboring unit cell geometries leads to an unstable frequency response.

Keywords: Frequency selective surface, FSS, periodic structures, incidence angle, stability

Birim Hücreler Arası Mesafenin Frekans Seçici Yüzeylerin Frekans Kararlılığına Etkisi

Öz

Periyodik iletken geometriler literatürde frekans seçici yüzey (FSY) olarak adlandırılmaktadırlar. Geometrilerine bağlı olarak filtre davranışı sergileyen FSY'lerin frekans yanıtları geometrilerine, elektromanyetik dalganın geliş açısına, frekansına ve polarizasyonuna bağlıdır. Periyodik iletken geometriler arasındaki mesafe FSY'lerin en önemli parametrelerinden birisidir ve frekans cevabı üzerine olan etkisi literatürde bugüne kadar yeterince araştırılmamıştır. Bu çalışmada dört farklı FSY geometrisi seçilerek periyodik iletken geometriler arasındaki mesafenin FSY'lerin frekans kararlılığı üzerine olan etkisi incelenmiştir. Seçilen FSY geometrilerinin benzetimleri Ansoft HFSS yazılımı tarafından gerçekleştirilmiş ve oldukça ilginç bir sonuç elde edilmiştir. Periyodik iletken geometriler arasındaki mesafe "0.1" rezonans dalga boyunun altına düşürüldüğünde beklenenin aksine FSY'in geliş açısı kararlılığının önemli ölçüde azaldığı görülmüştür. Literatürde birim hücre boyutu azaldıkça FSY'lerin frekans kararlılıklarının arttığı ifade edilmektedir. Periyodik iletken geometriler arasındaki mesafe "0.1" rezonans dalga boyunun altına düştüğünde, komşu hücrelerin iletken yolları arasında meydana gelen girişimler baskın hale gelmekte ve FSY'in kararsız frekans yanıtına sahip olmasına yol açmaktadır.

Anahtar Kelimeler: Frekans seçici yüzey, FSY, periyodik yapılar, geliş açısı, kararlılık

*dokenb@itu.edu.tr
Bora DÖKEN, https://orcid.org/0000-0002-1874-3844

1. Introduction

Periodic conductive geometries that exhibit filtering behaviour are referred to as frequency-selective surfaces (FSSs) in the literature. The frequency response of FSSs depends on their geometries, the angle of incidence, frequency, and polarization of the incoming electromagnetic wave (Munk, 2000). Radomes (Costa and Monorchio, 2012; Narayan et al., 2018), microwave ovens, absorber surfaces (Li et al., 2012), parabolic antennas (Brandão et al., 2017), and reduction of the interference between wireless communication systems (Sung et al., 2006; Döken and Kartal, 2017; Yang et al., 2020; Yin et al., 2018; Barros et al., 2017) are some of the application areas of FSSs. Most of these applications require stable frequency response against the changes in the angle of incidence of the electromagnetic wave. Multiple FSS structures have been proposed to achieve a stable frequency response (Yan et al., 2015; Zhao et al., 2016; Azemi, Ghorbani, and Rowe, 2015). The common feature of these works is the proposal of various methods to reduce the FSSs' unit cell sizes. A miniaturized FSS that is angularly stable up to 60 degrees of incidence angles is presented in (Varuna, Ghosh, and Srivastava, 2016). In (Mingbao et al., 2014), an anchor-shaped FSS with dual-band stopping behaviour is proposed, which exhibits excellent miniaturization with "0.065λ x 0.076λ", where "λ" represents the free-space wavelength of the resonance frequency. In (Kartal, Golezani, and Doken, 2017), a hybrid FSS geometry is proposed to achieve multiple stopbands and stable frequency response in small cell sizes.

The frequency responses of FSSs are achieved by executing commercial electromagnetic simulators. The equivalent circuit (EC) models, based on the approximation of the frequency-selective surface as a lumped circuit, are mostly used in the literature to reveal the relationships between the frequency responses and the parameters of FSSs (Langley and Parker, 1982; Using et al., 2017; Fallah, Ghayekhloo, and Abdolali, 2015). EC models are valid up to the frequency at which grating lobes occur (Munk, 2000). In (Borgese and Costa, 2020), the higher-order first harmonic Floquet effect is considered by including an additional lumped element. In (Costa, Monorchio, and Manara, 2012), the transmission and reflection characteristics of FSSs are evaluated using a simple and accurate first-order circuit approach. This work also analyses and models the oblique incidence effect on the impedance of the frequency-selective surface.

FSSs are defined by various parameters depending on their geometries. Among these parameters, the distance parameter (“g” in Figure 1) between periodic conductor geometries is essential. However, the effect of this parameter on the frequency stability of FSSs has not been sufficiently investigated to date, except the work in (Costa, Monorchio, and Manara, 2012), which analyses and models the oblique incidence effect on the impedance of the frequency-selective surface.

This study aims to investigate the effect of the distance (g) (Figure 1) between unit cell geometries on the frequency response of FSSs. Four different FSS geometries are selected for this purpose. Simulations of these FSS geometries were carried out by Ansoft HFSS software. The EC model is also used to determine the relationship between its parameters and the frequency response of FSS.

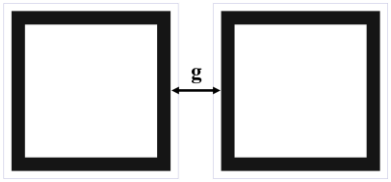

Figure 1. The distance (g) between unit cell geometries.

2. Materials and Methods

In this work, four different FSS geometries, shown in Figure 2, are employed to reveal the effect of the "g" parameter on the frequency response of FSSs: Square Loop (SL), Circle Loop (CL), Four-Legged Loaded (FLL), and Modified Four-Legged Loaded (MFLL). These well-known loops typed FSS geometries have almost stable frequency responses and their resonant wavelengths are almost equal to the length of their circumferences [7].

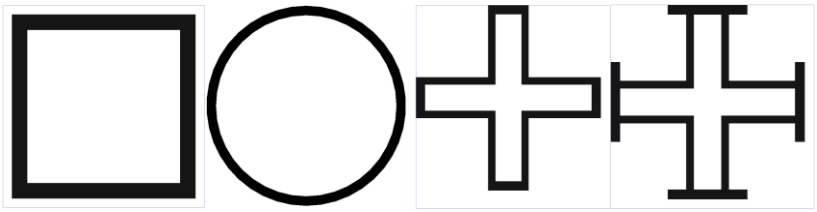

(a) (b) (c) (d)

Figure 2. a) Square Loop b) Circle Loop c) Four-Legged Loaded d) Modified Four-Legged Loaded.

EC model is efficiently used in the design and optimization stages of this work to determine the effect of the parameters of the FSS on its frequency response. As an example, a single-resonance band-stop FSS geometry and its EC model are shown in Figure 3. The arrow next to $\vec{E}$ denotes the direction of electric field lines in Figure 3. The equivalent capacitance ($C \propto \frac{w}{g}$) is defined by the width of the gap (w) and the distance (g) between periodic element geometries, while the equivalent inductance ($L \propto \frac{d}{w}$) is defined by the length (d) and width (w) of the current path. Since the FSS behaves like a metal wall when its impedance approaches zero, the resonance frequency of the FSS is derived as shown in Eq.1. As it is clear from Eq. 1, the resonant frequency of the FSS depends on its geometrical parameters.

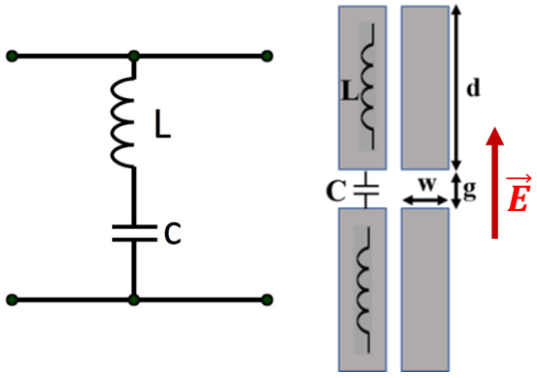

(a) (b)

Figure 3. A sample FSS and its EC.

$$f_r \approx \frac{1}{2\pi\sqrt{LC}} \quad (1)$$

In the first stage of this work, the resonance frequency of each FSS geometry is optimized in the 2.5-3.5 GHz frequency band while maintaining the unit cell dimensions to be close to each other. Therefore, FSSs' incident angle behaviour is not affected by the dimensions of the unit cells. In the second stage of the work, the incident angle stability of FSS geometries is researched by simulating the FSS geometries for different incidence angles ang “g” parameter values.

3. Results and Discussion

In the first stage of this work, the resonance frequency of each FSS geometry is optimized in the 2.5-3.5 GHz frequency band while maintaining the unit cell dimensions to be close to each other. The achieved unit cell dimensions and resonant frequencies for TE polarization at normal incidence angle for 1 mm spacing between unit cells (*g*) are SL (21 mm, 2.42 GHz), CL (21.4 mm, 3.10 GHz), FLL (21 mm, 2.89 GHz), and MFLL (21 mm, 2.48 GHz). The resonant frequency of the CL geometry occurs at a higher frequency due to the shorter conductor path length.

In the second stage of the work, the FSS geometries are simulated from normal to 50 degrees of incidence angles (θ) at TE (Transverse Electric) and TM (Transverse Magnetic) polarizations. Significant conclusions are revealed from the achieved simulation results.

The average ratio of the difference between the resonance frequencies at “g=2 mm” and “g=0.1 mm” to the resonance frequency for “g=2 mm” is given in Table 1 for each FSS geometry. The average ratios were calculated from all incidence angle results. Variation of resonant frequencies with respect to “g” values for normal incidence angle is also given in Figure 4. The FSS geometries in this work are symmetrical with respect to the "x" and "y" axis and their simulation results for normal incidence angle are same for TE and TM polarizations. Therefore, only TE polarization results are given in Figure 4. As shown in Table 1 and Figure 4, achieved resonance frequencies are significantly reduced with the decrease of "g" values at all polarizations. This issue can easily be expressed by using EC theory. As the distance between unit cell geometries decreases, the equivalent capacitance increases and resonance frequency decreases (Eq. 1). As expected, the maximum change in resonant frequency occurs at the SL geometry due to having maximum equivalent capacitance value between unit cell geometries.

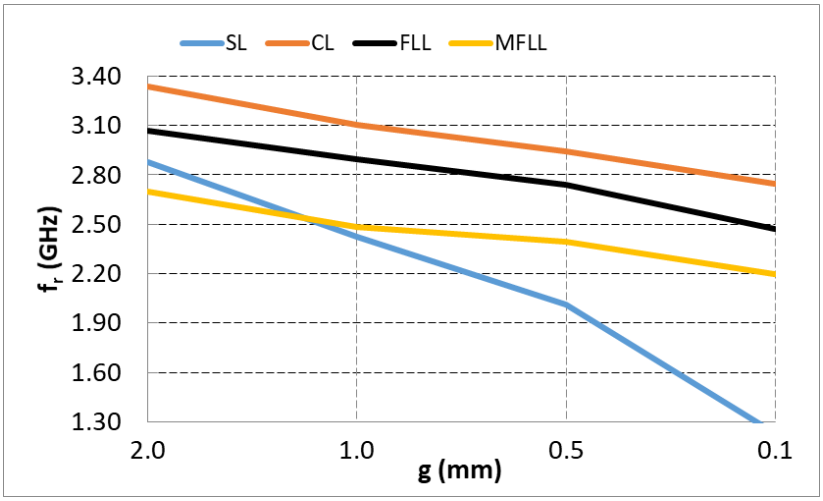

Figure 4. Variation of resonant frequency with "g" values ($\theta=0^0$, TE polarization).

Table 1: The average ratio of the change in resonance frequency between "g=2 mm" and "g=0.1 mm" to the resonance frequency for "g=2 mm": $(f_{g=2mm} - f_{g=0.1mm})/f_{g=2mm.}$

TE RL	TE CL	TE FLL	TE MFLL	TM RL	TM CL	TM FLL	TM MFLL
55.11%	16.89%	15.44%	19.39%	56.04%	16.92%	19.11%	23.48%

The resonance wavelengths corresponding to the "g" parameter values for each FSS geometry are denoted in Table 2. According to the results in Table 2, 0.1 mm of "g" value is less than 1% of the resonance wavelengths, and the 2 mm of "g" value is approximately equal to the value of 2% of the resonance wavelengths.

Table 2: The resonance wavelength correspondence value of the "g" parameter at $\theta=0^0$.

	TE 2mm	TE 1mm	TE 0.5mm	TE 0.1mm	TM 2mm	TM 1mm	TM 0.5mm	TM 0.1mm
RL	1.92%	0.81%	0.34%	0.04%	1.92%	0.82%	0.33%	0.04%
CL	2.22%	1.03%	0.49%	0.09%	2.23%	1.03%	0.49%	0.09%
FLL	2.05%	0.97%	0.46%	0.08%	2.05%	0.97%	0.46%	0.08%
MFLL	1.80%	0.83%	0.40%	0.07%	1.80%	0.83%	0.40%	0.07%

Achieved transmission (S21) resonance frequencies with respect to incidence angles are given in Figures 5-12 for "g" parameter values between 0.1 mm to 2 mm at TE polarization. It is clear from the simulation results that the frequency response of the FSS is unstable when the "g" value is less than 0.1% of the resonance length. On the other hand, when the "g" value approaches 2% of the resonance length, the change in the frequency response of the FSS becomes almost stable and sudden changes in resonant frequency do not appear.

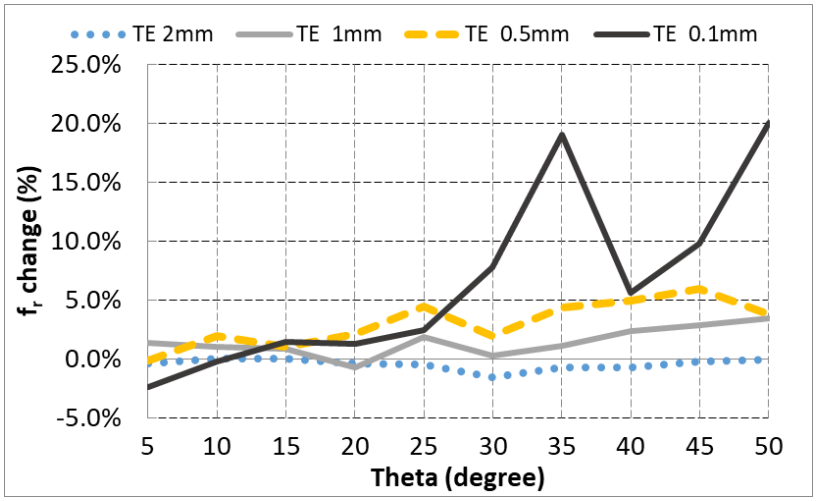

Figure 5. The variations in resonance frequencies for different incidence angles (SL, TE polarization).

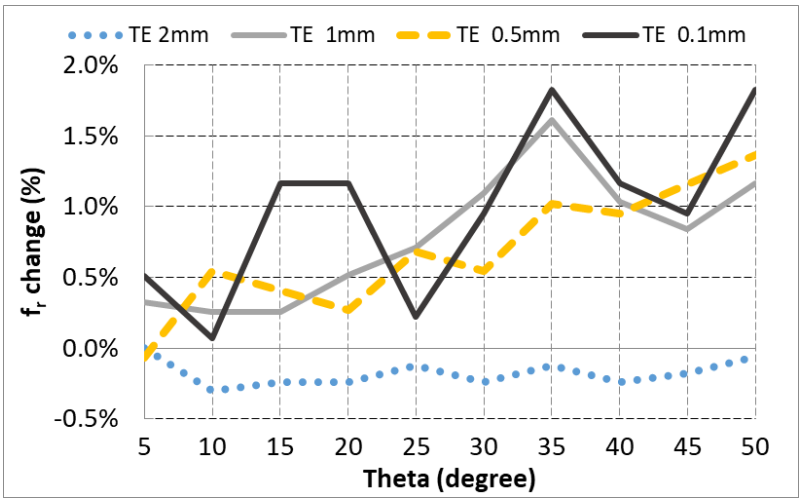

Figure 6. The variations in resonance frequencies for different incidence angles (CL, TE polarization).

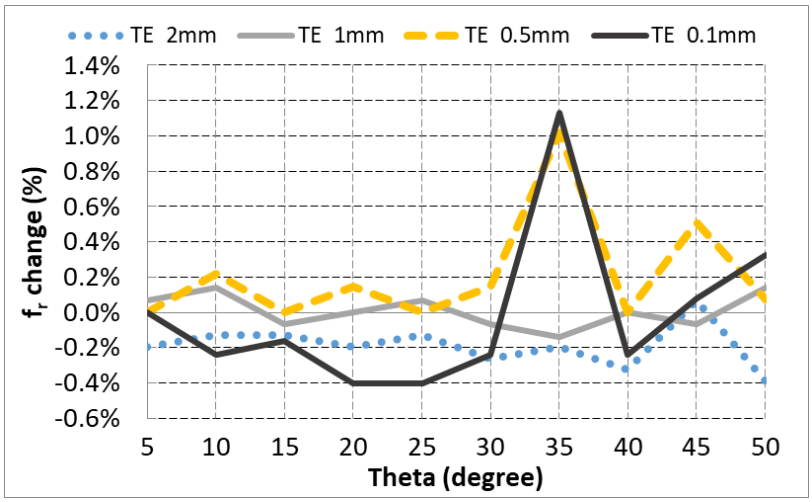

Figure 7. The variations in resonance frequencies for different incidence angles (FLL, TE polarization).

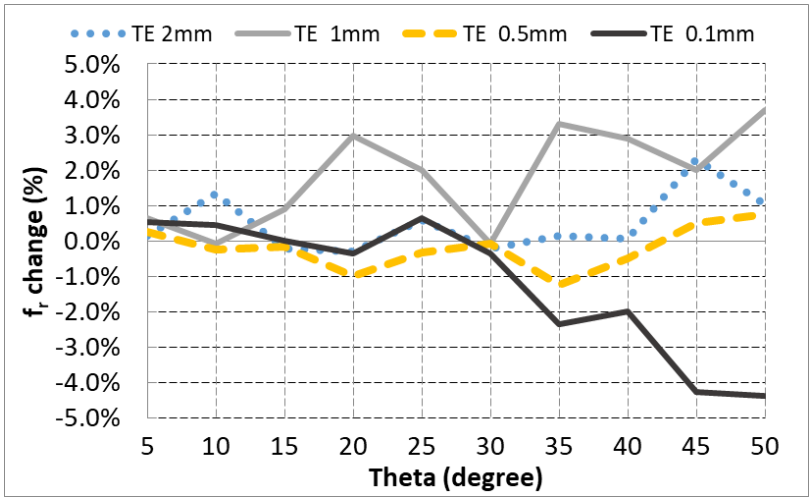

Figure 8. The variations in resonance frequencies for different incidence angles (MFLL, TE polarization).

According to the simulation results in Figures 9-12, the resonance frequencies increase with the increase of incidence angle at TM polarization. This issue can easily be expressed by using EC theory. The stored electric field energy between unit cells decreases with the increase of the incidence angle at TM polarization, which leads to decreased equivalent capacitance values. As a result, resonance frequency increases (Eq. 1).

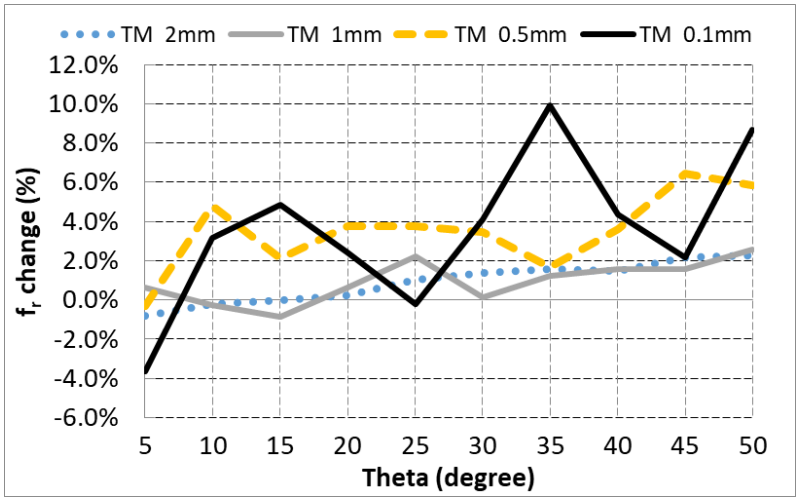

Figure 9. The variations in resonance frequencies for different incidence angles (SL, TM polarization).

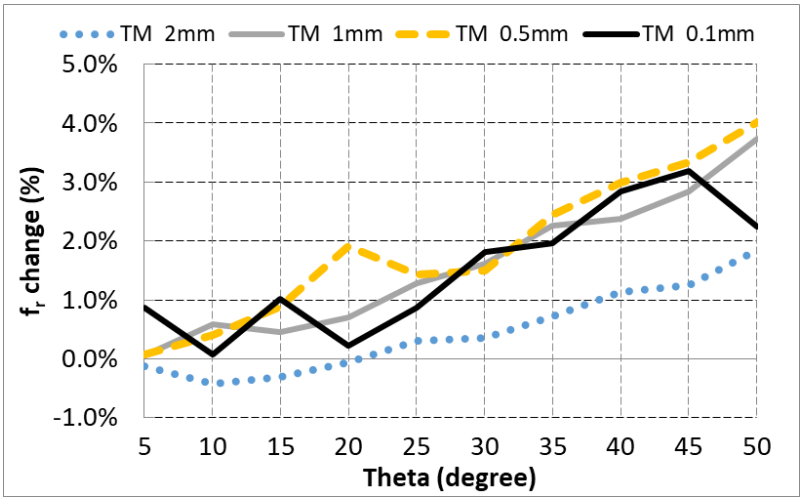

Figure 10. The variations in resonance frequencies for different incidence angles (CL, TM polarization).

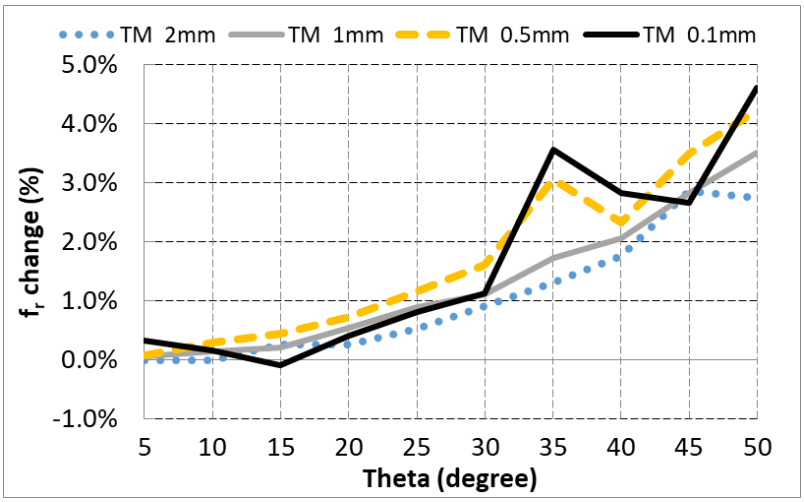

Figure 11. The variations in resonance frequencies for different incidence angles (FLL, TM polarization).

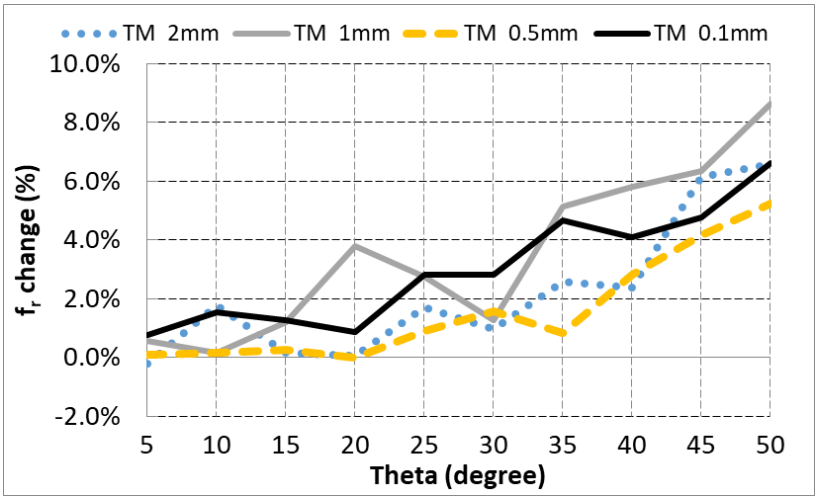

Figure 12. The variations in resonance frequencies for different incidence angles (MFLL, TM polarization).

The ratio of the maximum change in resonance frequency between 0-50 degree of incidence angles ($f_{max\_\Delta\theta} - f_{\theta=0}$) to the normal incidence resonance frequency ($f_{\theta=0}$) is given in Table 3.

The results in Table 3 are the mathematical summary of the results achieved from Figures 5-12. In this table, the instability of the resonance frequencies for the value of g=0.1 mm is clear.

Table 3: The ratio of the maximum resonance frequency variation between 0-50 degrees of incidence angles to normal incidence: $(f_{max\_\Delta\theta} - f_{\theta=0})/f_{\theta=0}$.

	TE 2mm	TE 1mm	TE 0.5mm	TE 0.1mm	TM 2mm	TM 1mm	TM 0.5mm	TM 0.1mm
RL	1.56%	2.85%	5.96%	19.01%	2.18%	2.20%	6.46%	9.90%
CL	0.30%	1.61%	1.16%	1.82%	1.25%	2.84%	3.33%	3.20%
FLL	0.33%	0.14%	1.02%	7.52%	2.87%	2.83%	3.50%	3.56%
MFLL	2.30%	3.30%	1.25%	4.27%	6.13%	6.36%	4.17%	4.77%

4. Conclusion

The most crucial result revealed in this study is that the distance ("*g*") between periodic conductor geometries significantly affects the incidence angle stability of the FSS. An interesting result is revealed that the angle stability of the FSSs deteriorates as the "g" parameter decreases. As the value of the "g" parameter decreases, the unit cell size of the FSS decreases. It is known from the FSS theory that the incidence angle stability increases as the unit cell size decreases. This result does not coincide with the general theory of FSS. The incidence angle stability of the observed FSSs greatly decrease when the "g" value is almost reduced below 0.1% of the resonance wavelength. The observed "0.1%" resonance wavelength value varies according to the type of FSS geometry and its parameters. However, it can be specified that the decrease in the distance between the periodic geometries increases the interference effect between the conductor geometries. Consequently, as the angle of incidence of the electromagnetic wave changes, the interference at different places of neighbouring unit cell geometries leads to unstable frequency response. This issue should be considered during the design phase of FSSs.

Ethics in Publishing

There are no ethical issues regarding the publication of this study.

Author Contributions

Bora Döken: Designing the study, performing the calculations, evaluating the results, writing the article

References

Azemi, S. N., Ghorbani, K., & Rowe, W. S. T. (2015). Angularly Stable Frequency Selective Surface With Miniaturized Unit Cell. *Ieee Microwave and Wireless Components Letters*, *25*(7), 454–456.

Barros, V. F., Silva Segundo, F. C. G. da, Campos, A. L. P. S., Silva, S. G. da, & Gomes Neto, A. (2017). A novel simple convoluted geometry to design frequency selective surfaces for applications at ISM and UNII bands. *Journal of Microwaves, Optoelectronics and Electromagnetic Applications*, *16*(2), 553–563.

Borgese, M., & Costa, F. (2020). A simple equivalent circuit approach for anisotropic frequency-selective surfaces and metasurfaces. *IEEE Transactions on Antennas and Propagation*, *68*(10), 7088–7098.

Brandão, T. H., Filgueiras, H. R. D., Cerqueira, S. A., Mologni, J. F., & Bogoni, A. (2017). FSS-based dual-band cassegrain parabolic antenna for RadarCom applications. *2017 SBMO/IEEE MTT-S International Microwave and Optoelectronics Conference (IMOC)*, 1–4.

Costa, F., & Monorchio, A. (2012). A frequency selective radome with wideband absorbing properties. *IEEE Transactions on Antennas and Propagation*, *60*(6), 2740–2747.

Costa, F., Monorchio, A., & Manara, G. (2012). Efficient analysis of frequency-selective surfaces by a simple equivalent-circuit model. *IEEE Antennas and Propagation Magazine*, *54*(4), 35–48.

Döken, B., & Kartal, M. (2017). Easily Optimizable Dual-Band Frequency Selective Surface Design. *IEEE Antennas and Wireless Propagation Letters*, *16*, 2979–2982.

Fallah, M., Ghayekhloo, A., & Abdolali, A. (2015). Design of frequency selective band stop shield using analytical method. *Journal of Microwaves, Optoelectronics and Electromagnetic Applications*, *14*(2), 217–228.

Kartal, M., Golezani, J. J., & Doken, B. (2017). A Triple Band Frequency Selective Surface Design for GSM Systems by Utilizing a Novel Synthetic Resonator. *IEEE Transactions on Antennas and Propagation*.

Langley, R. J., & Parker, E. A. (1982). Equivalent circuit model for arrays of square loops. *Electronics Letters*, *18*(7), 294–296.

Li, M., Xiao, S., Bai, Y.-Y., & Wang, B.-Z. (2012). An ultrathin and broadband radar absorber using resistive FSS. *IEEE Antennas and Wireless Propagation Letters*, *11*, 748–751.

Mingbao, Y., Shaobo, Q., Jiafu, W., Jieqiu, Z., Hang, Z., Hongya, C., & Lin, Z. (2014). A Miniaturized Dual-Band FSS With Stable Resonance Frequencies of 2.4 GHz/5 GHz for WLAN Applications. *IEEE Antennas and Wireless Propagation Letters*, *13*, 895–898. https://doi.org/10.1109/lawp.2014.2320931

Munk, B. A. (2000). *Frequency Selective Surfaces - Theory and Design*. John Wiley and Sons. Inc. internal-pdf://84.134.66.94/FSS Teory and Design Book.pdf

Narayan, S., Gulati, G., Sangeetha, B., & Nair, R. U. (2018). Novel metamaterial-element-based FSS for airborne radome applications. *IEEE Transactions on Antennas and Propagation*, *66*(9), 4695–4707.

Sung, G. H. H., Sowerby, K. W., Neve, M. J., & Williamson, A. G. (2006). A frequency-selective wall for interference reduction in wireless indoor environments. *IEEE Antennas and Propagation Magazine*, *48*(5), 29–37. https://doi.org/10.1109/Map.2006.277152

Using, A., Resonators, L. C., Zhang, K., Jiang, W., & Gong, S. (2017). Design Bandpass Frequency Selective Surface. *IEEE Antennas and Wireless Propagation Letters*, *16*, 2586–2589.

Varuna, A. B., Ghosh, S., & Srivastava, K. V. (2016). An Ultra Thin Polarization Insensitive

and Angularly Stable Miniaturized Frequency Selective Surface. *Microwave and Optical Technology Letters*, *58*(11), 2713–2717.

Yan, M., Qu, S., Wang, J., Zhang, A., Zheng, L., Pang, Y., & Zhou, H. (2015). A Miniaturized Dual-Band FSS With Second-Order Response and Large Band Separation. *IEEE Antennas and Wireless Propagation Letters*, *14*, 1602–1605. https://doi.org/10.1109/lawp.2015.2413942

Yang, Y., Li, W., Salama, K. N., & Shamim, A. (2020). Polarization Insensitive and Transparent Frequency Selective Surface for Dual Band GSM Shielding. *IEEE Transactions on Antennas and Propagation*, *69*(5), 2779–2789.

Yin, W., Zhang, H., Zhong, T., & Min, X. (2018). A novel compact dual-band frequency selective surface for GSM shielding by utilizing a 2.5-dimensional structure. *IEEE Transactions on Electromagnetic Compatibility*, *60*(6), 2057–2060.

Zhao, P. C., Zong, Z. Y., Wu, W., & Fang, D. G. (2016). A Convoluted Structure for Miniaturized Frequency Selective Surface and Its Equivalent Circuit for Optimization Design. *IEEE Transactions on Antennas and Propagation*, *64*(7), 2963–2970.